Optimal compensation capacitors maximizing coreless inductive power transfer

Yohan Wanderoild, Adrien Morel, Romain Grézaud, Gaël Pillonnet, Dominique Bergogne, Hubert Razik

Optimal compensation capacitors maximizing coreless inductive power transfer.

Yohan Wanderoild[1], Adrien Morel[1], Romain Grezaud[1], Gael Pillonnet[1], Dominique Bergogne[1], Hubert Razik[2]
[1]Univ, Grenoble Alpes, F-38000 Grenoble, France
CEA, LETI, Minatec Campus F-38054 Grenoble, France
[2] Universite Claude Bernard Lyon 1, AMPERE UMR CNRS 5005, Villeurbanne, France
Contact: yohan.wanderoild@cea.fr

Abstract

The use of coreless transformers is still limited because of the power they can transmit and the reactive power they absorb. This paper introduces a comprehensive theoretical approach of the transferable power and the related compensation topologies allowing to optimize the system used. Analytical equations are given in order to estimate the maximum power transmission of a coreless transformer. Based on the theoretical results the optimal topology can then be selected accordingly to the power source, the transformer and the sensibility over the deviations of the elements. This methodology has been validated experimentally and allowed to transmit 2W through a 2.25cm² coreless transformer under 1 MHz. Moreover this results can be broaden to any inductive power transfer system.

Introduction

Coreless transformers also known as coupled coils, allow to transmit power without any physical link, making them the perfect candidates for inductive power transfer (IPT). Indeed, this technology is currently being standardized for electrical vehicle chargers or biomedical implants. Furthermore, the transmission of energy through a magnetic field without a magnetic core allow the system to work at high temperature, high frequency while simplifying the fabrication process. As it also ensure a galvanic isolation, it appears to be an excellent solution for high temperature, high frequency isolated power converters [1], [2].

1. Fundamentals of inductive power transfer

Firstly, we are going to introduce the fundamental differences between a transformer with or without a magnetic core.
In magnetic core transformers, as explained by Witulski [3], the use of a ferromagnetic core allows to drastically reduce the magnetic energy stored, since the magnetic permeability of the air is drastically lower than the magnetic material one. As a matter of fact, the magnetizing inductor L_m in Fig. 1 is several decades lower for coupled coils than in a transformer with a magnetic core. Moreover, without the use of a magnetic core, the magnetic field is no longer channeled between the two coils. It significantly decreases the coupling between the two coils and thus the magnetizing

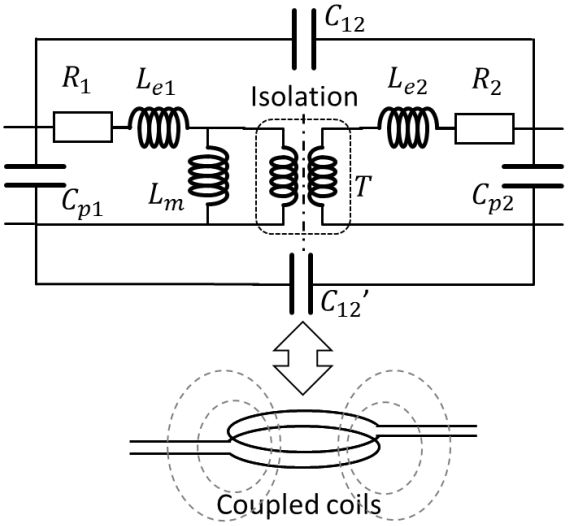

Fig.1 Conventional model of coreless transformers (T; ideal transformer).

inductor, at the cost of an increase of the leakage inductors identified as L_{e1} and L_{e2} in Fig. 1.

Consequently, without proper compensation, the low magnetizing inductor L_m sinks a lot of current and adversely affects the power transfer from the primary to the secondary side. This inductor stores a significant amount of reactive power which needs to be compensated through harmonics oscillators. This compensation is made thanks to capacitors adequately tuned to the system.

In order to correctly adjust the compensation, the parasitic couplings need to be taken into account. If the working frequency is too close to the self-resonating frequency of the transformer, the interwinding coupling due to the electrostatic coupling between tracks can be substantial enough to affect the compensation. These capacitors which depend on the design of the transformer can be approximated by $C_{\mathrm{p1}}, C_{\mathrm{p2}}$ and C_{12}. For simplicity purposes the analytic solutions given are not taking into account these capacitances but the comprehensives solutions can be calculated using the same methodology.

A coreless transformer not only needs a significant amount of reactive energy, it also consumes active energy. The losses due to the copper, the current crowding and the skin effect must also be considered. These losses can be modeled by the frequency dependent resistances $R_1$and R_2.

The reactive power sunk by the transformer through the magnetizing inductor L_m is conventionally compensated with two impedance converters (Fig. 2.).

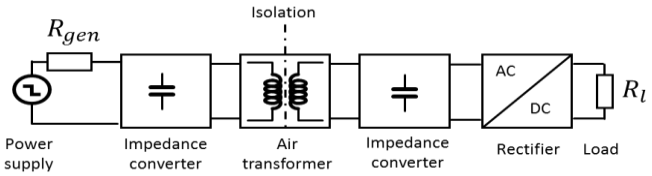

Fig. 2 Conversion chain based on a coreless transformer.

The impedance converters are set to maximize the available output power, they can be made with a serial or a parallel capacitor forming the four possible topologies shown in Fig. 3.

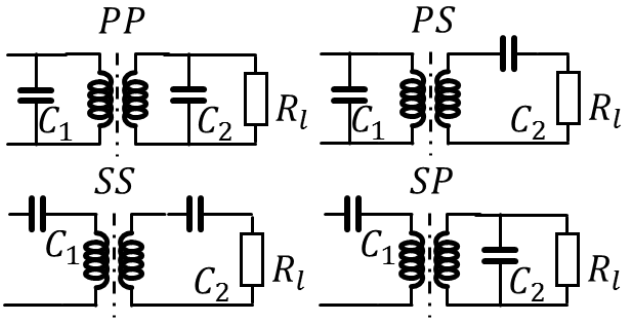

Fig. 3 Conventional compensation topologies

The selection of the topology and associated components have been several time emphasized in literature. Wang's [4] and Auvigne [5] have presented methodologies which are available only when the losses modeled by $R_1$and R_2 are negligible. in Fig. 1 are negligible. Wu [6] and Helpern [7] have shown solutions for highly resistive transformers but only for SS and SP topologies.

This paper provides a new approach compatible with highly resistive transformers and generators for the four conventional topologies with their respective optimal load value.

2. Theoretical maximum power achievable

Based on an accurate model, the compensation can be optimized and the output power correctly estimated. First of all it is important to note that we are working with resonating oscillator, hence the compensation is valid at a given working frequency. Shifting the latter would detune the converters.

Considering that the optimized transformer acts as a bandpass filter, the first harmonic analysis allows to have a good estimation of the output power. This presumption has been validated thanks to a transient analysis showing a maximum 10% error with the first order approximation as shown in table 3. The generator is modeled by a resistive equivalent source. The maximum power that may be transferred can be calculated with a proper impedance matching and a Thevenin equivalent circuit composed by the generator, the primary impedance converter and the transformer as modeled in Fig. 4.

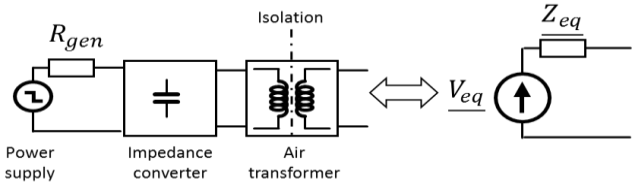

Fig. 4 Thevenin equivalent circuit of the first part of the conversion chain

For a given source and a given transformer, the values of $\underline{Z_{eq}}$ and $\underline{V_{eq}}$ are not affected by the load or the secondary impedance converter C_2, which mean that the equivalent model of the source is only dependent of value of C_1.

This equivalent source can provide a limited power level to the secondary converter and the load C_2 and R_l which must be chosen to absorb as much power as possible from the upstream conversion chain. Thanks to the maximum power theorem we can estimate the maximum power deliverable by the equivalent source constituted by $\underline{Z_{eq}}$ and $\underline{V_{eq}}$ to the secondary. The maximum power transmission is obtained when the load modeled by $\underline{Z_{load}}$, is perfectly matched to the source (1).

$$\underline{Z_{eq}}^{*} = \underline{Z_{load}}. \tag{1}$$

When (1) is respected, the maximum power transmitted to the secondary P_{max} can expresses with $\underline{Z_{eq}}$ and $\underline{V_{eq}}$ regardless of the load and the secondary impedance converter.

$$P_{max}(C_1) = \frac{V_{eq}^2(C_1)}{4 \cdot Re\left(Z_{eq}(C_1)\right)} \tag{2}$$

Therefore C_1 can then be chosen by solving (3) in order to maximize the power transmitted.

$$\frac{\partial P_{max}}{\partial C_1} = 0 \tag{3}$$

The load R_l associated with the secondary impedance converter C_2 are then chosen in order to respect (1).

For ease of reading, these shorted variables will be used.

$$Z_{L_1} = L_m\omega + L_{e1}\omega$$

$$Z_{L_m} = L_m\omega$$

$$R_{g1} = R_{gen} + R_1$$

For a serial primary compensation, SS and SP topologies, the optimal value of C1 is given by

$$C_1 = \frac{1}{Z_{L_1}\omega} \tag{4}$$

For a parallel primary compensation, PP & PS topologies the optimal value of C1 is given by

$$C_1 = \frac{Z_{L_1}}{({Z_{L_1}}^2 + \frac{R_1}{R_2}{Z_{L_m}}^2 + {R_1}^2)\omega} \tag{5}$$

If we consider that the power supply provides an rms tension V_{in}, for SS and SP topologies the maximum power given by the equivalent source is:

$$P_m = \frac{Vin^2}{4R_{g1}\left(1 + \frac{R_2 R_{g1}}{{Z_{L_m}}^2}\right)} \tag{6}$$

For PP and PS topologies, the maximum power becomes:

$$P_m = \frac{Vin^2\left(\left({Z_{L_1}}^2 + {R_1}^2\right) + \frac{R_1}{R_2}{Z_{L_m}}^2\right)}{4\left[\frac{A^4 R_2}{{Z_{L_m}}^2} + A^2\left(R_1 + R_{g1}\right) + {Z_{L_m}}^2\frac{R_1}{R_2}R_{g1}\right]} \tag{7}$$

Where $A^2 = {Z_{L_1}}^2 + R_1 R_{g1}$

The secondary compensation is then calculated in order to match the equivalent source. When a rectifier is used, it can be modeled with the first harmonic approximation, as shown in Fig. 5.

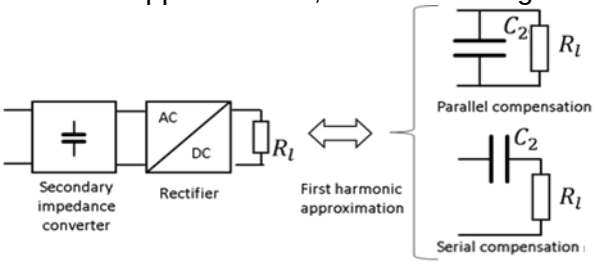

Fig. 5 Secondary impedance converter equivalent model.

In order to match the equivalent source, for a serial secondary compensation, SS and PS topologies the load and the impedance converter are given by

$$C_2 = \frac{1}{-Im(\underline{Z_{eq}}) \cdot \omega} \qquad R_l = Re(\underline{Z_{eq}}) \tag{10}$$

For a parallel secondary compensation, SP and PP topologies the optimal values become

$$R_l = Re(\underline{Z_{eq}}) \cdot (1 + \left(\frac{Im(\underline{Z_{eq}})}{Re(\underline{Z_{eq}})}\right)^2) \quad (11)$$

$$C_2 = \frac{Im(\underline{Z_{eq}})}{\omega * (Re(\underline{Z_{eq}})^2 + Im(\underline{Z_{eq}})^2)} \quad (12)$$

A combination between a parallel and a series compensation allows to have more flexibility regarding the optimal load.

Topology choice

The choice of the secondary compensation has no effect on the output power available as expressed by (2). It can be proven mathematically by comparing (6) and (7) that serial compensation for the primary side will be able to provide more power if the condition given by (13) is respected.

$$R_{gen}{}^2 < Z_{L1}^2 + \frac{R_1}{R_2} Z_{Lm}{}^2 + R_1{}^2 \quad (13)$$

In most cases the power source is less resistive than the transformer, making the serial compensation for the primary the ideal choice for maximizing the power transferred.

In addition, the primary compensation has a clear effect on the current drown by the converter. On the one hand, the serial compensation avoids DC current passing through the transformer. On the other hand, when the converter is supplied by a square source, the voltage transient can create a substantial current peak in the parasitic and compensation capacitances. As a result, this may stress the source and increase drastically the losses in the converter, and, as a consequence lower the efficiency of the whole conversion chain. This current peak is due to the low impedance seen by the source at high frequency.
In the case of a parallel primary compensation the power source will be directly connected to the capacitance which will drain high frequency currents. Nevertheless, in the case of a serial primary the high frequency currents are stopped by the primary L_{e1} and L_m, although it may pass though the interwinding capacitance $Cp1$.

This phenomenon can be avoided by using a sinusoidal source, or by adding shock inductors between the generator and the impedance converter, this would increase the impedance seen by the power source at high frequency. However the primary compensation capacitance would have to be changed accordingly and the output power would be affected by the losses in the added inductors.

Finally it must be pointed out that the sensibility over the choice of the impedance converter's elements values changes according to the generator, transformer and the topology chosen. For example, for the primary impedance converter unlike the parallel compensation the optimal value of C_1 for a serial compensation is independent of the coupling and R_1 and R_2. It can be also noted that the parallel primary capacitor has no effect as long as the generator used presents a negligible impedance in front of the one of the compensated transformer. The sensibility analysis allows to choose the topology in order to adapt the converter to the physical constraint and to focus the attention on the choice of the key components.

Transformer characterization

To validate the proposed methodology, the PCB coreless transformer shown in Fig 6 has been used.
The primary as well as the secondary have been made with 18 square turns on two layers. The copper tracks are 17µm thick and 200 µm width and 150 µm isolation between each turn. The primary and secondary are separated with 710 µm of FR4.

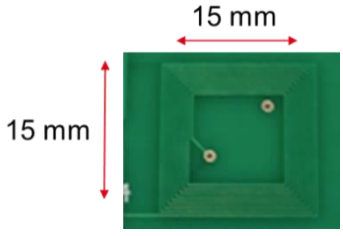

Fig. 6 Transformer used for experimental validation of the proposed design methodology

In order to perfectly tune the matching elements the transformer used has been measured with a Keysight E4990A impedance analyzer.

C_{12}. is determined by shorting the primary and the secondary and measuring the impedance between the two.
An algorithm has then been applied in order to match the model with the measurement of the impedance of the transformer with open and short secondary. The open secondary measurement presents two peaks, which is a direct consequence of the bifurcation phenomena [4]. In our case, the first peak is due to the resonating RLC circuit composed of C_1, L_{e1}, L_m then the second peak is mainly due to the RLC composed of $C_1, C_2, C_{12}, L_{e1}, L_{e2}$.
To consider the skin effect, the resistors have been modeled by $R = R_0 + R_{skin} \cdot \sqrt{f}$. The estimated values can be found in Table 1. The real part of the impedance measured being several decades lower than the imaginary part at the working frequency, the resistive values are difficult to measure. The measurement of the resistive parts would be improved by tuning the resonant devices at the working frequency.
Keeping in mind that the current crowding effect is linked to the current passing through the magnetizing inductor, meaning that the values of the model's elements are dependent on the source and the load.

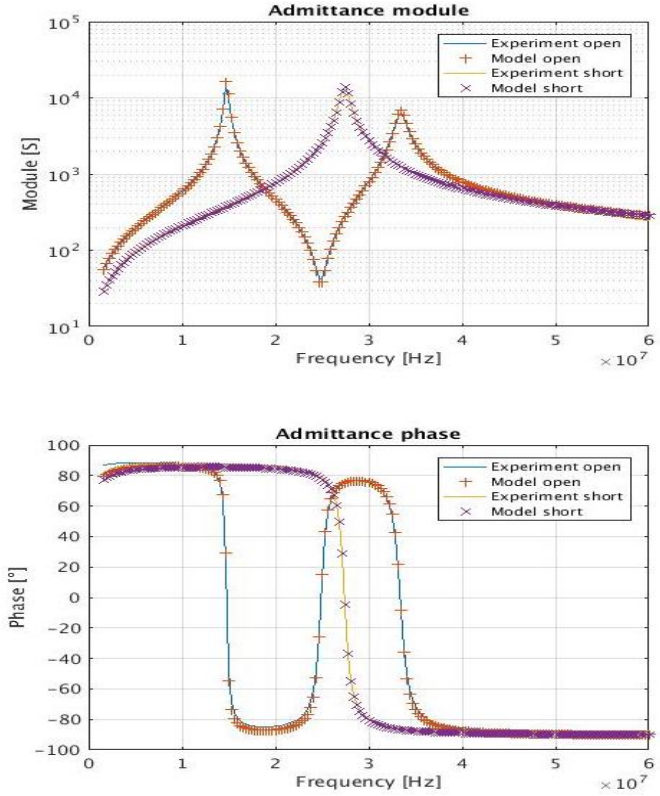

Fig. 7 Results of the matching algorithm between the model and the measurements.

Element	Value	Unit
R_1	1,5+0,002$\sqrt{f}$	Ω
R_2	1,5+0,002$\sqrt{f}$	Ω
L_{e1}	1,3	µH
Le_2	2,53	µH
L_m	4,25	µH
C_1	11	pF
C_2	11	pF
C_{12}	8,2	pF

Table.1 Estimated values for the model (Fig.1)

Experimental validation of the proposed method.

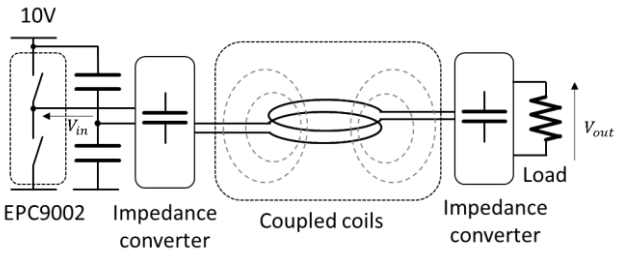

Fig. 8 Experimental set up

To compare the compensations methods, a square wave generator has intentionally been used as drawn in fig. 8.
To ensure that the good impedance converters and load have been placed, the impedance of the loaded compensated transformer has been measured and then compared to the simulation.
For each topology the calculated capacitance has been welded and adjusted thanks to a comparison with the simulation. During the tests, the conversion chain has been supplied with an EPC9004 development board under 1MHz. The capacitances and load used are given in Table 2.

	SS	SP	PS	PP	unit
C_1	4.56	4.56	2.84	2.84	nF
C_2	3.99	0.156	7.16	6.72	nF
R_l	197	205	5.66	92.8	Ω

Table 2 Values calculated and used for the compensation with each topology

The first harmonic analytic analysis has been validated with a transient simulation and experimental measurements (table 3).
An error lower than 7% has been noticed between the simulations. The discrepancy is due to the harmonics neglected in the analytical analysis.
The compensated transformer act as a bandpass filter. Unlike the SS topology, the PP topology allow a part of the current to pass through the capacitor without passing through the resistors R_1 and R_2, increasing the quality factor of the filter formed. As a result, the SS topology allows more harmonics to pass through the transformer and the output waveform display stronger harmonics than the others topologies as seen on Fig 9 and 10
The experimental measurements are showing an output power up to 33% lower. This discordance is due to a mismeasurement of the coils resistors, and the lack of current crowding simulation.

	SS	SP	PS	PP	
First harmonic simulation	3.02	3.02	1.17	1.17	W
Transient simulation	3.30	3.00	1.12	1.16	W
	6.6	0.7	4	0.8	%
Experiment	2.02	2.02	0.85	0.99	W
	33	33	27	15	%

Table 3 Output power and error vs first harmonic simulation for first harmonic simulation (proposed methodology), circuit simulation and measured for each topology.

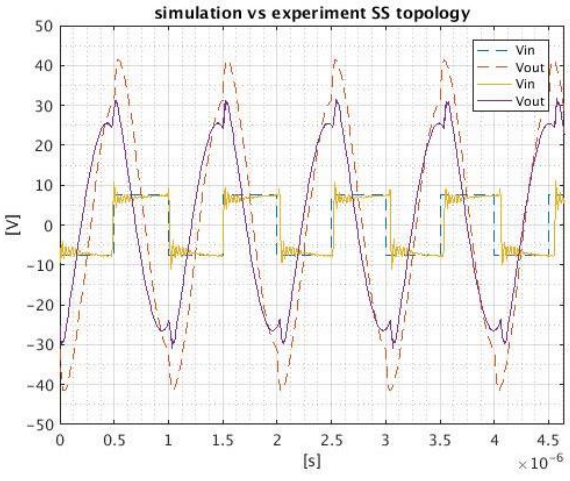

Fig. 9 Experiment and numerical simulation (dashed) of the SS topology

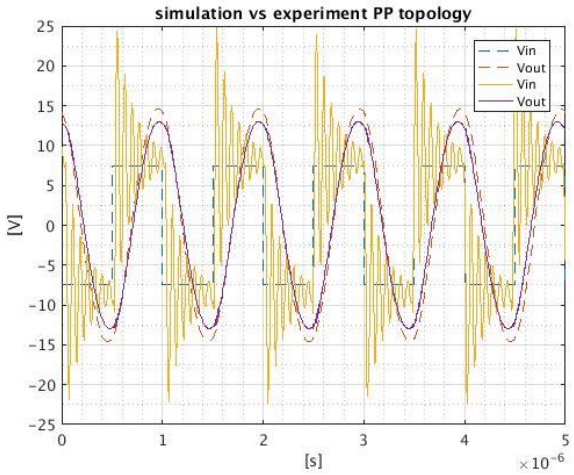

Fig. 10 Experiment and numerical simulation (dashed) of the PP topology

The measure of the current passing through the primary has been done on the characterized and compensated transformer, as expected the normalized frequency spectrum (Fig 11) present for the PS topology a richer frequency spectrum at 10 MHz. The transformer with a parallel compensation at the primary possesses a much lower input impedance at high frequency as shown on Fig. 12. These harmonics in the current absorbed by the transformer are increasing the losses within the power chin without increasing the output power. With a parallel compensation the strong current peaks induced are creating strong oscillation of the power source as seen on Fig. 10.

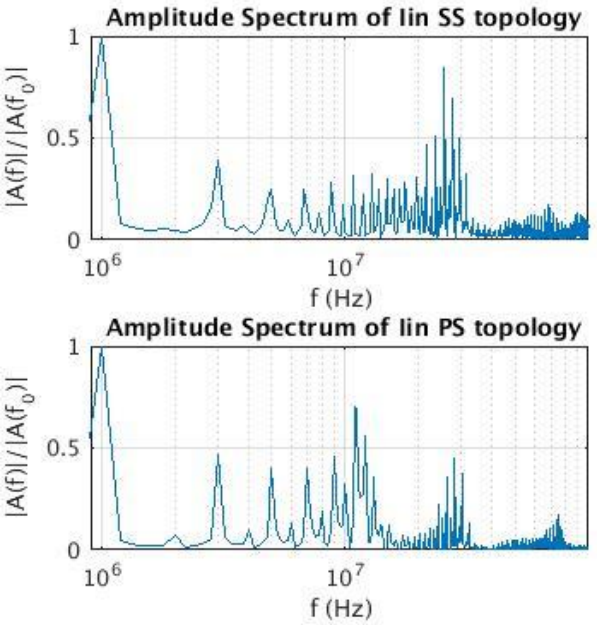

Fig. 11 frequency spectrum of the current measured

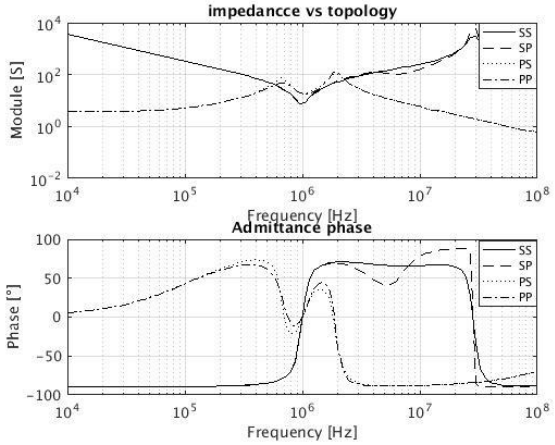

Fig. 12 Impedance seen by the power source obtained by simulation with the converter tuned at 1MHz

Conclusion

For a given transformer the maximum transferable power can be calculated. In order to reach this power an addition of two impedance converters is required. The choice of compensation used for the primary side impact the output power, but also the current draw by the system. Knowing the transformer and the source used, the optimal compensation can be calculated thought equation (13).

Using the proposed methodology and models, 2W has been transferred through a 2.25cm² coreless transformer under 1MHz, with a parasitic capacitance between the primary and secondary lower than 10pF.

Knowing the maximum output power delivered by a given transformer, an optimization can easily be done during the earliest stages of the transformer design can be easily done.

Since we are using a resonant compensation, the slightest variation of several parameters can drastically affects the power delivered. These variations can be created by production fluctuation, temperature changes, coupling with surrounding materials or by the current crowding phenomena. A sensibility analysis seems to be a key element in developing a closed loop approach to industrial production and will be investigated in our future works.

References

[1] Y. Wanderoild, D. Bergogne, and H. Razik, “High Frequency, High Temperature designed DC/DC Coreless Converter for GaN Gate Drivers,” *PCIM Eur. 2016*, 2016.

[2] D. Bergogne *et al.*, “Integrated coreless transformer for high temperatures design and evaluation,” in *2013 15th European Conference on Power Electronics and Applications (EPE)*, 2013, pp. 1–8.

[3] A. F. Witulski, “Introduction to modeling of transformers and coupled inductors,” *IEEE Trans. Power Electron.*, vol. 10, no. 3, pp. 349–357, May 1995.

[4] C.-S. Wang, G. A. Covic, and O. H. Stielau, “Power transfer capability and bifurcation phenomena of loosely coupled inductive power transfer systems,” *IEEE Trans. Ind. Electron.*, vol. 51, no. 1, pp. 148–157, Feb. 2004.

[5] C. Auvigne, P. Germano, Y. Perriard, and D. Ladas, “About tuning capacitors in inductive coupled power transfer systems,” in *2013 15th European Conference on Power Electronics and Applications (EPE)*, 2013, pp. 1–10.

[6] H. H. Wu, A. P. Hu, S. C. Malpas, and D. M. Budgett, “Determining optimal tuning capacitor values of TET system for achieving maximum power transfer,” *Electron. Lett.*, vol. 45, no. 9, pp. 448–449, Apr. 2009.

[7] M. E. Halpern and D. C. Ng, “Optimal Tuning of Inductive Wireless Power Links: Limits of Performance,” *IEEE Trans. Circuits Syst. Regul. Pap.*, vol. 62, no. 3, pp. 725–732, Mar. 2015.